Computer Science and Information Systems 00(0):0000–0000 https://doi.org/10.2298/CSIS260411051W

Paper Type: Research Paper

Enhancing Image Classification with Multi-Data-Per-Qubit Processing: A High-Efficiency Quantum Convolutional Scheme

Xiaoliang Wang[1,2], Lianghai Chen[1], Yi Lu[1], Liang Bai[1], Huaning Song[2], and Kuanching Li[1]

[1] School of Computer Science and Engineering, Hunan University of Science and Technology, China
{fengwxl, liangbai77}@hnust.edu.cn,
chenlh@mail.hnust.edu.cn, aliric@hnust.edu.cn (corresponding author),
24010502004@mail.hnust.edu.cn
[2] School of Artificial Intelligence and Manufacturing, Hechi University, China
shn_2008@163.com (corresponding author)

Abstract. As an emerging research direction in quantum computing, quantum convolutional neural networks provide a promising way to combine quantum feature processing with traditional machine learning algorithms; however, their development is constrained by the scarcity of quantum resources. In this work, we propose a quantum-classical hybrid convolutional neural network model based on quantum convolution kernels. This model employs a multi-data-per-qubit rotation-angle encoding scheme to embed multiple data points into a small number of qubits, aiming to reduce quantum resource consumption and enhance feature extraction for image classification tasks. Its compact structure is designed to extract multidimensional features with fewer qubits and reduced measurement overhead, thereby improving the utilization of limited quantum resources under the considered setting. To evaluate our method, we conducted several experiments to compare our model with existing approaches and to assess performance under varying numbers of qubits, different CNOT gate configurations, and diverse encoding schemes. Experimental results show that the proposed model achieves competitive performance and slightly higher average accuracy than the traditional convolution structure and three existing quantum convolution schemes under a Qiskit Aer noisy simulation environment. This investigation provides a compact design for the structural optimization and low-resource implementation of quantum convolutional neural networks, offering a potential scheme for quantum-assisted image feature extraction.

Keywords: Quantum Computing, Image Classification, Quantum Circuits, Quantum Machine Learning (QML), Quantum Convolutional Neural Networks.

1. Introduction

Deep learning has achieved remarkable results in image classification tasks [1,2,3]; however, its model parameters are large and training energy consumption is high, revealing bottlenecks in computing efficiency and scalability [4,5,6]. In this context, quantum

computing is seen as a potential route to break through the bottleneck of traditional image processing [7]. In particular, quantum machine learning models based on parameterized quantum circuits or quantum annealers have shown unique advantages in extracting high-dimensional features and nonlinear mapping [8,9]. However, in the current "noisy medium-scale quantum" stage, hardware limitations such as the limited number of qubits, the short coherence time, and the high quantum gate error rate still severely restrict the actual deployment of QML models [10,11,12]. Therefore, it is significant to carry out resource-efficient model design and optimization research to address hardware bottlenecks, enhancing the practical application of quantum machine learning.

Inspired by the research introduced in [13], this work optimizes the classical data encoding process from the coding and circuit architecture perspective, redesigns the quantum circuit, and proposes an innovative quantum-classical hybrid convolutional neural network architecture. The core of this architecture is to design the quantum computing unit as a parameterized circuit specifically for performing image feature extraction, while the traditional computing unit is responsible for the subsequent classification task. This model uses a rotation-angle encoding strategy based on repeated R_Y rotations to handle image classification problems. Compared with the conventional computational basis encoding method, this strategy reduces the required number of qubits for local image-block processing. Unlike circuit architectures in which the number of qubits is directly tied to the number of data points to be processed, the proposed design allows multiple normalized data values to be sequentially embedded into a smaller number of qubits through structural optimization. Although the R_Y rotations change the amplitudes of quantum states, the input data are encoded as rotation angles rather than through conventional amplitude encoding.

To evaluate the effectiveness of our model, we conducted experiments on IBM's Qiskit quantum experimental platform and performed a 10-class image classification task on the MNIST dataset. The experimental results show that the QC-CNN model achieves competitive classification performance while using a compact quantum circuit design, indicating its potential applicability under limited quantum resources. In addition, in our experiments, we also studied the performance of our model under different encoding gates, entanglement gates, and the number of qubits to gain a deeper understanding of the properties and effectiveness of our model.

The main contributions of this research are as follows:

1. To present a novel hybrid quantum Convolutional Neural Network (QC-CNN) designed for multi-class image classification. The model is designed to capture critical image features by leveraging quantum circuits and demonstrates competitive classification accuracy under the current experimental setting.
2. To propose a compact quantum convolution layer, which reduces the use of quantum gates and qubits in the circuit and simplifies the model structure through circuit-level optimization.
3. To investigate the relationship between the number of qubits and the number of convolution data, and propose a convolution circuit that performs convolution processing on multiple data with a small number of qubits.

The remainder of this article is as follows. Section 2 introduces the basic concepts of quantum computing, and Section 3 presents related work in machine learning using quantum computing. Section 4 details the structure of our model. Section 5 provides a

comprehensive experimental evaluation of the model's performance. Section 6 investigates the scalability and computational efficiency of the proposed approach, and finally, concluding remarks and future work are depicted in Section 7.

2. Background

As the most basic discrete unit in the material world, a quantum has unique physical properties that provide a new paradigm for information processing. Unlike classical physical systems, quantum systems exhibit non-classical characteristics such as superposition and entanglement, which lay the physical foundation for building new computing architectures. In quantum computing, qubits constitute the basic unit of information processing, essentially different from binary bits in classical computing.

The uniqueness of qubits is that their quantum states can be expressed as a linear superposition of two orthogonal ground states (usually denoted as $|0\rangle$ and $|1\rangle$), as shown in Eq. (1). In the mathematical expression of this superposition state, the complex coefficients α and β represent the quantum amplitudes of the corresponding ground states, respectively, whilst the squares of their moduli ($|\alpha|^2$ and $|\beta|^2$) represent the probability that the quantum state collapses to the corresponding ground state when measured. This probabilistic measurement result reflects the basic principles of quantum mechanics and is an essential feature distinguishing quantum computing from classical computing. The superposition state of qubits is not a simple probability mixture, but contains the core characteristic of quantum coherence, which provides a physical basis for quantum parallel computing.

$$|\psi\rangle = \alpha\,|0\rangle + \beta\,|1\rangle\,, \quad |\alpha|^2 + |\beta|^2 = 1, \quad \alpha, \beta \in \mathbb{C} \tag{1}$$

Another crucial property is entanglement. When two or more qubits are in an entangled state, non-local correlations are formed between them. Even if they are far apart in space, the measurement result of one quantum bit will instantly affect the state of other qubits. This correlation cannot be explained by classical probability theory, and the entangled state cannot be decomposed into a simple tensor product of the states of individual qubits. Specifically, for a two-body system, its entangled state $|\Psi_{AB}\rangle$ cannot be expressed in the form of $|\psi_A\rangle \otimes |\psi_B\rangle$ (where $\otimes$ represents a tensor product operation), which reflects the non-local and indivisible characteristics of quantum entanglement.

In the process of implementing quantum computing, the quantum circuit model is one of the most widely used frameworks and consists of three interconnected parts.

2.1. Information Coding

In quantum computing, the input of any quantum algorithm is represented in the form of quantum states, so classical data must first be converted into corresponding quantum states. At present, common quantum data encoding methods mainly include computational basis coding and amplitude coding. Computational basis coding is achieved by mapping classical data to the ground state of the quantum system. It is usually necessary to first convert the classical data into a binary representation and then express it with the corresponding quantum ground state. Amplitude coding uses the amplitude of the quantum state to carry classical data information, so the data needs to be normalized to ensure

that the sum of the squares of all amplitudes is equal to 1. Based on these coding strategies, researchers have proposed a variety of methods to achieve quantum state representation of image data [14].

$$R_X(\theta)\text{ Gate} = \begin{bmatrix} \cos\frac{\theta}{2} & -i\sin\frac{\theta}{2} \\ -i\sin\frac{\theta}{2} & \cos\frac{\theta}{2} \end{bmatrix} \qquad R_Y(\theta)\text{ Gate} = \begin{bmatrix} \cos\frac{\theta}{2} & -\sin\frac{\theta}{2} \\ \sin\frac{\theta}{2} & \cos\frac{\theta}{2} \end{bmatrix}$$

$$R_Z(\theta)\text{ Gate} = \begin{bmatrix} e^{-i\theta/2} & 0 \\ 0 & e^{i\theta/2} \end{bmatrix} \qquad H\text{ Gate} = \frac{1}{\sqrt{2}}\begin{bmatrix} 1 & 1 \\ 1 & -1 \end{bmatrix} \qquad \text{CNOT Gate} = \begin{bmatrix} 1&0&0&0 \\ 0&1&0&0 \\ 0&0&0&1 \\ 0&0&1&0 \end{bmatrix}$$

Fig. 1. Matrix representations of the $R_X(\theta)$, $R_Y(\theta)$, $R_Z(\theta)$, H, and CNOT gates.

2.2. Quantum State Transformation

The core of quantum computing lies in the evolution of quantum states, which play a vital role in a variety of computing tasks. After the classical information is mapped to the quantum state, several quantum gates are needed to manipulate the qubits to achieve state conversion. The quantum gate changes the initial quantum state through operations such as rotation and entanglement to meet subsequent computing needs. Unlike classical logic gates, quantum gates must satisfy unitary properties to ensure the normalization characteristics of the quantum system and the reversibility of the evolution to avoid information loss. The basic quantum gates involved in this article include: RX gate, RY gate, RZ gate, CNOT gate, H gate, and others. The matrix representation of these quantum gates is shown in Fig. 1.

2.3. Measuring Quantum States

The quantum circuit concludes with a measurement process that transforms quantum state information into classical data. The resulting expectation value, representing the quantum computation outcome, is utilized in this work as a feature representation of the input image, enabling subsequent classification analysis. Regarding QML, PQC is often used as a hybrid method, such as [15,16,17]. PQC consists of fixed quantum gates, and the change of quantum states and the entanglement of information are realized through the cooperation between quantum gates.

3. Related Work

Although quantum hardware still has certain technical limitations, applying quantum computing to image classification has become a research hotspot and has attracted more

and more attention. This section briefly reviews the relevant research, first introducing the research progress of quantum machine learning and quantum neural networks, then exploring the performance of quantum convolutional networks in image processing.

3.1. Quantum Machine Learning

In recent years, Quantum Machine Learning (QML) has witnessed significant advances, particularly in understanding quantum models' generalization behavior and expressive capabilities. For instance, [18] investigated the generalization properties of QML models under limited training data and revealed that the generalization error can be effectively minimized when only a small subset of parameterized quantum gates undergo substantial updates during training. This insight offers theoretical support for model compression and complexity control within quantum learning frameworks. Motivated by these theoretical developments, [19] proposed the Quantum Implicit Representation Network (QIREN), which generalizes Fourier Neural Networks (FNNs) to the quantum regime. QIREN demonstrates strong performance in various tasks, including signal representation, super-resolution, and image synthesis, thereby showcasing the potential of QML for compact and efficient data modeling. At the same time, progress has also been made in exploiting quantum algorithms for practical advantages. For example, Caro et al. [18] presented a quantum algorithm based on bilateral correlation for distributed machine learning under communication constraints, as their method enables efficient solutions to least-squares fitting and Soft-max regression problems, with extensibility to tasks such as Hamming distance computation, thereby emphasizing the strengths of quantum algorithms in communication-limited environments. In terms of quantum system optimization and resource efficiency, Pan et al. [19] proposed a quantum coupon collection protocol that combines coherent states and linear optics, and experimentally verified that it can significantly reduce sample collection overhead, providing a practical reference for how to use limited resources in quantum algorithm design effectively. Recent studies in quantum machine learning have shown the potential of quantum methods in improving communication efficiency and demonstrating task-specific quantum advantage [20,21]. [22] further studied the problem of automatic quantum architecture search (QAS), constructed a unified evaluation benchmark covering 900 random quantum circuits and 400 unitary matrices, and compared six mainstream optimization algorithms, providing a systematic evaluation framework and standard for quantum neural network structure search.

3.2. Quantum Neural Networks

In the study of quantum neural networks, Zhou et al. [23] and Meng et al. [24] proposed representative models and methods. Based on single-bit operation and measurement and using the decoherence effect induced by the environment, Zhou et al. [23] constructed a new quantum neural network model, which reduced the difficulty of physical implementation and showed good nonlinear classification ability and noise resistance, promoting the development of early quantum neural computers. Similarly, Meng et al. [24] proposed the Residual Matrix Product State (ResMPS) structure from the perspective of combining tensor networks and neural networks. On the basis of retaining the efficient modeling ability

of tensor networks, nonlinear activation and random deactivation mechanisms were introduced to improve the stability and expression ability of the model, and the interpretability of the model was enhanced under the theoretical framework of polynomial expansion.

Wu et al. [25] explored the data parallelism problem in quantum neural networks, and for the first time realized parallel data processing using quantum superposition and entanglement, and strictly proved that under orthogonal coding, parallel training and separate training are equivalent in terms of loss function. These studies have promoted the integration of quantum computing and neural networks from different perspectives. Among them, Zhou et al. [23] and Meng et al. [24] focused on the basic theory of quantum neural networks, and Wu et al. [25] studied the problem of data parallelism. Recent studies have explored hybrid quantum-classical convolutional neural networks for image classification, demonstrating the potential of quantum convolutional structures to enhance feature extraction and recognition performance [26,27]. These works enrich the theoretical system of QML and provide necessary guidance for subsequent research.

Beyond directly related QML studies, recent AI-driven modeling works also provide useful references for feature representation, temporal dependency modeling, and complex classification tasks. Okmi et al. [28] reviewed mobile phone data in crime applications and summarized data types, analytical perspectives, and challenges in real-world data-driven modeling. Ku et al. [29] demonstrated the use of LSTM-based models for stock market prediction, showing the importance of temporal feature modeling in complex sequential data. He et al. [30] further introduced an attention-based trans-LSTM framework for epileptic seizure detection, highlighting the role of attention mechanisms and feature integration in improving representation ability. Taherinavid et al. [31] investigated transportation mode classification using deep reinforcement learning with smartphone sensors, providing a complementary example of learning-based classification under heterogeneous sensor data. Although these works address different application domains, they collectively show that effective feature representation and task-specific model design are central issues in modern AI-based classification, which is consistent with the motivation of the proposed compact quantum-classical feature extraction framework.

4. Methodology

This work proposes a Hybrid Quantum Convolutional Neural Network (QC-CNN) designed to classify images through supervised deep learning techniques. As illustrated in Fig. 2, the proposed model consists of four main components: 1) data processing, 2) quantum convolution layers, 3) measurement layer, and 4) dense layer. The quantum part of the model is expected to effectively extract significant features from the input images, while the classical part performs the final classification.

4.1. Data Processing

In the data preparation stage, the original graph data is first reduced in dimension to reduce computational complexity. Unlike traditional normalization methods [32], the proposed rotation-angle encoding process normalizes the input feature values to the interval $[0, \pi]$, enabling them to be directly used as rotation angle parameters for the quantum R_Y gate, thereby completing the encoding transformation from classical data to quantum states.

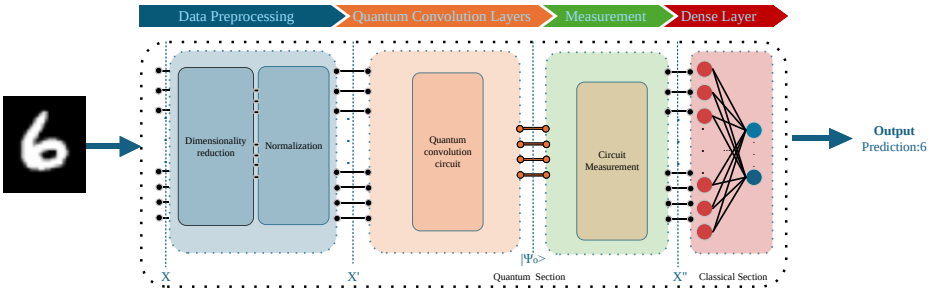


Fig. 2. Overall architecture of the model

4.2. Quantum Convolution Layers

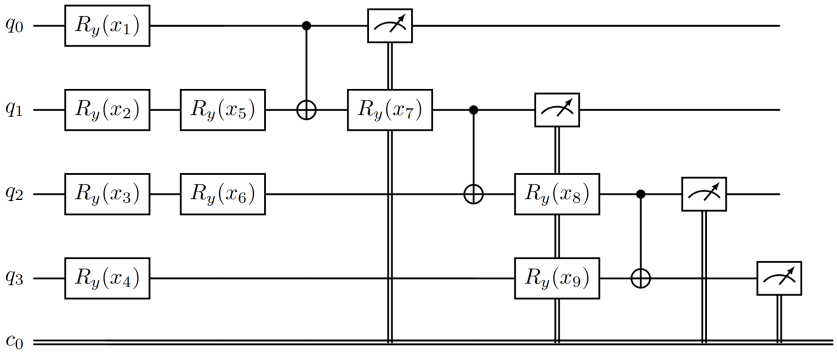


Fig. 3. Quantum convolution circuit

As illustrated in Fig. 3, the architecture consists of four quantum data qubits (q_0 to q_3) and a classical readout register. For each local 3×3 image region, the nine pixel values are first normalized and arranged in row-major order as x_1 to x_9. The first four values are encoded into q_0 to q_3 through R_Y rotation gates, while the remaining values are sequentially embedded through additional R_Y rotations placed between the entangling operations. In this sense, each rotation angle is data-dependent, and the circuit realizes a multi-data-per-qubit encoding mechanism rather than a one-pixel-one-qubit mapping. Entanglement among the qubits is achieved using a series of controlled-NOT (CNOT) gates arranged in a layered topology. The CNOT operations form a chain-like structure from q_0 to q_1, from q_1 to q_2, and from q_2 to q_3, allowing information to be progressively propagated across the four qubits. Additional R_Y rotations are applied between these entangling operations to enhance the circuit's expressiveness.

Measurements are performed on the four qubits in the computational basis, and the resulting classical outcomes are used to construct the feature vector for subsequent classical processing. The layered structure of encoding, entanglement, and measurement facilitates the extraction of high-dimensional and nonlinear features, which are crucial for downstream classification tasks.

Data Encoding In quantum computing, rotation gates are a class of single-qubit gates that rotate quantum states around specific axes on the Bloch sphere. The Pauli-Y rotation gate (R_Y gate) can be expressed as

$$R_Y(\theta) = e^{-i\frac{\theta}{2}Y} \tag{2}$$

where Y represents the Pauli-Y matrix:

$$\sigma_y = \begin{bmatrix} 0 & -i \\ i & 0 \end{bmatrix} \tag{3}$$

When the R_Y gate operates on the qubit states $|0\rangle$ or $|1\rangle$, its effects are as follows.
Operation on $|0\rangle$:

$$R_Y(\theta)\,|0\rangle = \cos\left(\frac{\theta}{2}\right)|0\rangle + \sin\left(\frac{\theta}{2}\right)|1\rangle \tag{4}$$

Operation on $|1\rangle$:

$$R_Y(\theta)\,|1\rangle = -\sin\left(\frac{\theta}{2}\right)|0\rangle + \cos\left(\frac{\theta}{2}\right)|1\rangle \tag{5}$$

Quantum Convolution In the QC-CNN framework, the quantum convolutional layer is designed to perform convolution operations, which are crucial for feature extraction and creating associated feature maps. Within this layer, the kernel size is set equal to the stride to efficiently down-sample the resulting feature maps. Similar to classical CNN architectures, these parameters should be adjusted on the basis of the input image dimensions. In implementing quantum convolution, the controlled-NOT gate (CNOT gate) plays an essential role in feature extraction and information transfer as a key two-qubit operation. The CNOT gate can create quantum entanglement, allowing information exchange among different qubits through quantum coherence, thereby achieving more efficient feature mapping. In addition, the CNOT gate is used in the quantum convolution layer to build correlations between quantum channels, so that features can be propagated between different qubits, thereby improving the expressiveness of the model. Compared with directly increasing the circuit size, this quantum processing structure may reduce circuit complexity and provide a compact feature representation under limited quantum resources.

The CNOT gate is a type of controlled gate that operates on two qubits: the control qubit and the target qubit. Its operation rule is as follows: if the control qubit is $|0\rangle$, the target qubit remains unchanged; if the control qubit is $|1\rangle$, the target qubit undergoes an X (NOT) transformation, i.e., $|0\rangle \leftrightarrow |1\rangle$.

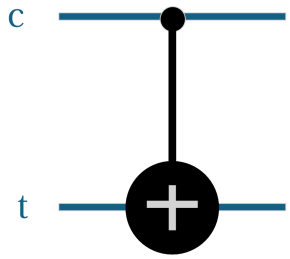


Fig. 4. CNOT gate

Mathematically, the operation of the CNOT gate can be expressed as

$$|c, t\rangle \rightarrow |c,\, t \oplus c\rangle \tag{6}$$

where c is the value of the control qubit, t is the value of the target qubit, and $\oplus$ represents the bitwise XOR operation.

In other studies, multiple CNOT gates are typically required. However, in our circuit design, only three CNOT gates are used to achieve entanglement between data qubits. These three CNOT gates connect four qubits, creating entanglement among them and enhancing the quantum circuit's expressive power for input data. In our convolution circuit, by strategically placing R_Y encoding gates at key positions, we enable four qubits to perform convolution on nine classical data points. This contrasts with other quantum convolution research, where the number of qubits must match the number of convolution data points.

Let the initial state of the four-qubit system be $|\psi_0\rangle = |0000\rangle$. First, we apply the R_Y rotation gates with rotation angles x_1, x_2, x_3, and x_4 to qubits q_0, q_1, q_2, and q_3, respectively. These operations encode the classical information into the quantum system and transform each qubit from the computational basis state into a superposition state:

$$|\psi_1\rangle = R_Y(x_1) \otimes R_Y(x_2) \otimes R_Y(x_3) \otimes R_Y(x_4)\, |\psi_0\rangle \tag{7}$$

Through the action of the R_Y gates, the amplitudes of the qubit states are adjusted, enabling the quantum system to represent the encoded classical features in a superposition form. This operation lays the foundation for subsequent feature interaction and entanglement construction.

Next, additional R_Y rotation gates with angles x_5 and x_6 are applied to qubits q_1 and q_2, respectively, to further enrich the encoded quantum features:

$$|\psi_2\rangle = I \otimes R_Y(x_5) \otimes R_Y(x_6) \otimes I\, |\psi_1\rangle \tag{8}$$

At this stage, the quantum states of q_1 and q_2 are further adjusted, allowing the circuit to increase the flexibility of feature representation before entanglement operations are introduced. Then, a CNOT gate is applied with q_0 as the control qubit and q_1 as the target qubit. This operation correlates the states of the two qubits and introduces quantum entanglement between them:

$$|\psi_3\rangle = \mathrm{CNOT}_{q_0 \rightarrow q_1}\, |\psi_2\rangle \tag{9}$$

After that, an $R_Y(x_7)$ rotation gate is applied to qubit q_1 to further transform its quantum state:

$$|\psi_4\rangle = I \otimes R_Y(x_7) \otimes I \otimes I \, |\psi_3\rangle \tag{10}$$

This rotation further adjusts the probability amplitudes of q_1, thereby influencing the subsequent entanglement propagation in the circuit.

Subsequently, another CNOT gate is applied, using q_1 as the control qubit and q_2 as the target qubit. This operation extends the correlation from the first pair of qubits to the next one:

$$|\psi_5\rangle = \mathrm{CNOT}_{q_1 \to q_2} \, |\psi_4\rangle \tag{11}$$

Next, the $R_Y(x_8)$ and $R_Y(x_9)$ rotation gates are applied to qubits q_2 and q_3, respectively, to further refine the encoded information and prepare the system for the final entangling operation:

$$|\psi_6\rangle = I \otimes I \otimes R_Y(x_8) \otimes R_Y(x_9) \, |\psi_5\rangle \tag{12}$$

These rotations provide additional data-dependent transformations for the lower two qubits, enhancing the expressive capacity of the circuit for feature extraction and nonlinear representation.

Finally, a third CNOT gate is applied with q_2 as the control qubit and q_3 as the target qubit, so that the entanglement is propagated through the four-qubit system:

$$|\psi_7\rangle = \mathrm{CNOT}_{q_2 \to q_3} \, |\psi_6\rangle \tag{13}$$

After these operations, the four-qubit system evolves from the initial basis state $|0000\rangle$ into a highly correlated quantum state that contains both superposition and entanglement. Finally, all qubits are measured to obtain the output of the quantum circuit. Through the above process, the circuit integrates classical data encoding, amplitude transformation, and hierarchical entanglement generation into a unified framework. The sequence of R_Y rotation gates allows the classical input features to be embedded into the amplitudes of the quantum states, while the chain of CNOT gates enables interactions among neighboring qubits. In this way, the circuit can effectively capture complex feature relationships and enhance the representation capability of the hybrid quantum-classical model.

4.3. Measurement Layer

The quantum measurement layer serves as the core module of the Quantum Convolutional Neural Network (QCNN), acting as a bridge from quantum state space to classical information space. It achieves efficient dimensionality reduction of quantum data while preserving key features through measurement techniques. This layer transforms quantum features extracted by the quantum convolutional layer into classically readable probability distributions using projective measurement, generalized measurement, or weak measurement, thereby supporting downstream tasks such as classification and regression. During this process, quantum measurement determines information extraction efficiency and directly affects the model's expressive power and computational efficiency through the synergistic effects of quantum state collapse and entanglement characteristics.

Let the measured observable A be a Hermitian operator, which can be expressed as

$$A = a_1 P_1 + a_2 P_2 + \cdots + a_n P_n \tag{14}$$

Suppose the quantum state of the system is

$$|\psi\rangle = c_1 |\varphi_1\rangle + c_2 |\varphi_2\rangle + \cdots + c_n |\varphi_n\rangle \tag{15}$$

The probability of measuring eigenvalue a_i is

$$P(a_i) = \langle\psi| P_i |\psi\rangle = |\langle\varphi_i|\psi\rangle|^2 \tag{16}$$

If the measurement result is a_i, the system collapses to the corresponding eigenstate:

$$|\psi'\rangle = \frac{P_i |\psi\rangle}{\sqrt{P(a_i)}} = |\varphi_i\rangle \tag{17}$$

After measuring the four qubits, we obtain four single-qubit measurement-related features as shown in Fig. 5. These four expectation values are passed to the subsequent classification layer through

$$F(P) = w_0 P_0 + w_1 P_1 + w_2 P_2 + w_3 P_3 + b \tag{18}$$

where w_i is the weight and b is the bias.

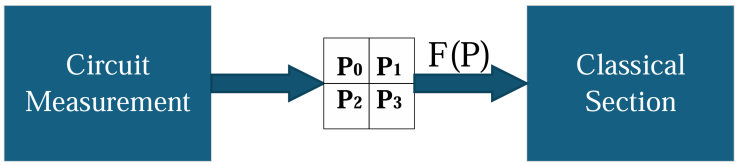


Fig. 5. F(P):Quantum data to classical data conversion

4.4. Dense Layer

After measuring the quantum layer, we input the results into the dense layer. This design is consistent with classical neural networks [33], where each input node is connected to each output node, and feature mapping is performed through a linear transformation (i.e., weighted summation plus bias) followed by a nonlinear activation function. The dense layer is typically used to extract global features and complete classification tasks, particularly at the network's back end to project high-dimensional features into the output space, such as a classification label probability distribution.

5. Experiments

To evaluate our model, we compared it with other models and conducted experiments to examine the effects of different factors on its performance. To comprehensively assess the effectiveness of the proposed model, we designed and carried out two types of experiments. The first type of experiment aimed to compare the overall performance differences

between the proposed model and multiple reference models in image classification tasks. The second type of experiment focused on the impact of the quantum circuit's characteristics on the model's performance, specifically including: (1) using different numbers of qubits for convolution operations, (2) introducing different numbers of CNOT gates in the circuit to adjust the entanglement strength, and (3) trying different classical data encoding methods (such as R_X, R_Y, etc.) to investigate their impact on feature expression ability.

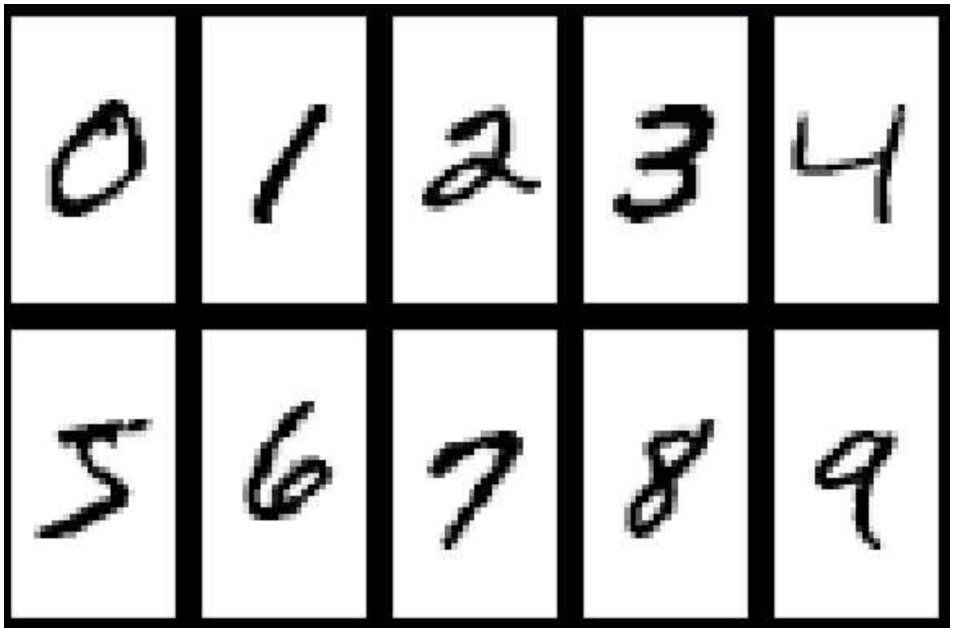


Fig. 6. MNIST dataset

In the first type of experiment to evaluate our proposed model's effectiveness, we selected three representative quantum models as comparison subjects. These models differ significantly from our proposed model in terms of circuit structure, encoding methods, and sequences of quantum gates.

QCNN1 [34] encodes classical data using R_Y gates and constructs quantum entanglement using CNOT gates. Its specific implementation is as follows: four qubits receive the encoded data through R_Y gates, respectively, and then CNOT gates are added successively between the 1st and 2nd qubits and between the 2nd and 3rd qubits for entanglement connection. In this experiment, $N = 2$ groups of the above structures are repeated to achieve quantum feature extraction of image blocks.

QCNN2 [15] uses a more specialized circuit structure, and its design sequence differs from the conventional quantum convolution method. This model first adds CNOT gates between the 1st and 2nd qubits as well as between the 3rd and 4th qubits to establish initial entanglement, then adds an extra CNOT gate between the 2nd and 3rd qubits to enhance information interaction, and finally encodes classical data into qubits through four R_Y gates.

QCNN3 [35] shows a more complex operation process in encoding and entanglement design. This model first completes data encoding for four qubits through R_Y gates and introduces R_X and R_Z gates on the 1st and 4th qubits, respectively, to enhance the state-space expression ability. Subsequently, by using the 3rd and 4th qubits as control qubits and the 2nd and 1st qubits as target qubits, two groups of CNOT gates are constructed to build an asymmetric entanglement structure.

The baseline QCNN models are reproduced according to their original circuit settings. Therefore, the comparison reflects the performance of representative circuit designs under the implemented experimental protocol, rather than a strictly identical circuit-depth or patch-size controlled comparison.

As shown in Fig. 6, this study employs the MNIST dataset as a standard benchmark for image classification tasks. Owing to its simple structure, ample sample size, and strong representativeness, MNIST has been widely adopted as a reference dataset for evaluating the performance and generalizability of quantum neural networks in numerous prior works [27,33,35]. Its discrete and low-resolution image format facilitates dimensionality reduction and quantum state encoding, making it especially suitable for simulation experiments under limited-qubit conditions. Accordingly, we adopt the MNIST dataset to assess the proof-of-concept effectiveness of the proposed Quantum Convolutional Neural Network (QCNN) model. Given the computational limitations of current quantum simulators, many studies have resorted to reducing dataset sizes to ensure feasibility [26]. For instance, [25] used 1,000 3×3 Tetris images, [15] employed 250 32×32 images for binary classification, and [23] conducted experiments on MNIST subsets. In line with this practice, we construct a class-balanced subset of the MNIST dataset, comprising 1,000 samples for training and 200 for testing in our 10-class classification task. Since this subset is relatively small, the results should be interpreted as a proof-of-concept evaluation of the proposed compact quantum convolution circuit rather than a complete demonstration of scalability to large-scale image classification tasks.

The proposed QCNN model is implemented and trained using IBM's Qiskit platform. To address a key limitation highlighted in [27]—namely, the common use of idealized quantum circuits without accounting for hardware noise—we incorporate Qiskit Aer's noise simulation into our experimental setup. This configuration not only improves the practical relevance of the results but also enables a more

more practical assessment of model performance than an ideal noiseless simulator. To mitigate the variability of quantum noise during circuit execution, we conduct multiple independent training runs for each model configuration and report averaged results. This approach reduces the influence of randomness in performance evaluation and improves the reliability of the observed trends.

In terms of experimental settings, we set the number of training epochs to 50 and the batch size to 64. The loss function is cross-entropy loss with label smoothing ($= 0.1$) to alleviate the problem of overfitting to the training samples. The Adam optimizer is used for parameter updates. The training process of each model is repeated three times under the same experimental protocol. The average and standard deviation of the three independent results are then calculated for subsequent comparative analysis.

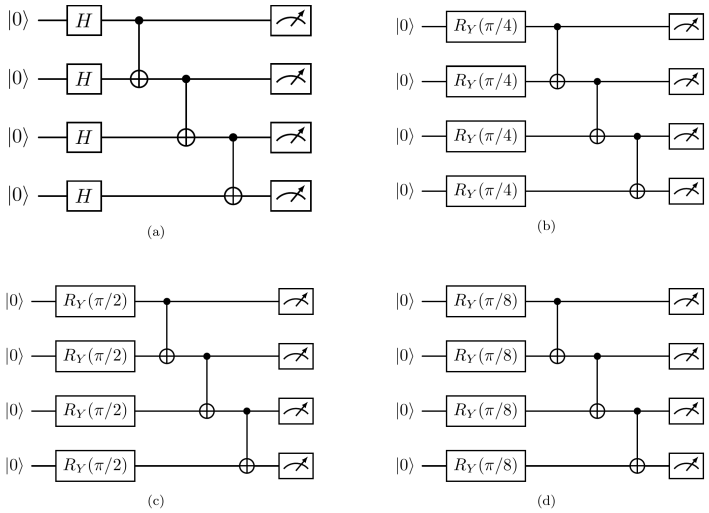


Fig. 7. Four quantum circuits for experimental environment noise evaluation

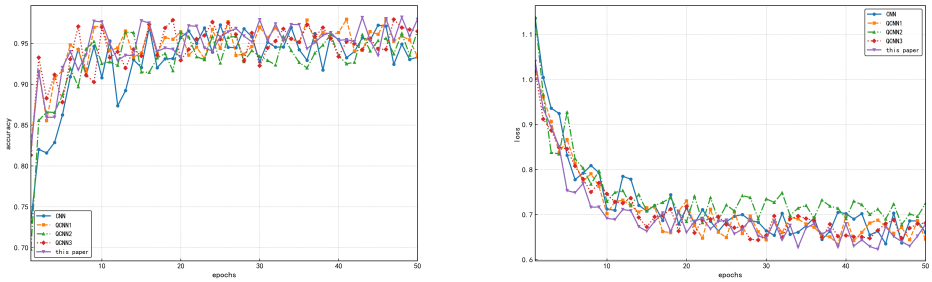
Table 1. Experimental environment noise assessment

qubit	a		b		c		d	
	Noisy	Ideal	Noisy	Ideal	Noisy	Ideal	Noisy	Ideal
1	0.492 ± 0.0276	0.5	0.1467 ± 0.0312	0.1464	0.5002 ± 0.0379	0.5	0.0612 ± 0.0085	0.38
2	0.4732 ± 0.0321	0.5	0.3220 ± 0.0265	0.25	0.5034 ± 0.0026	0.5	0.0872 ± 0.0124	0.073
3	0.5318 ± 0.0121	0.5	0.3156 ± 0.0329	0.3232	0.5206 ± 0.0428	0.5	0.1136 ± 0.0186	0.106
4	0.4957 ± 0.0263	0.5	0.3796 ± 0.0234	0.375	0.5249 ± 0.0305	0.5	0.1386 ± 0.0239	0.136

5.1. Performance Comparison

Table 2. Performance comparison of different models

model	qubit	gate	size	Accuracy
CNN	/	/	3×3	0.975
QCNN1	4	7	2×2	0.970854 ± 0.006114
QCNN2	4	14	2×2	0.960801 ± 0.003847
QCNN3	4	10	2×2	0.977291 ± 0.001770
this paper	4	12	3×3	0.978214 ± 0.002648



(a) accuracy **(b)** loss

Fig. 8. Classification performance comparison between the proposed model and others

We compared the proposed quantum convolution model with one classical baseline (CNN) and three reference quantum convolution models. The corresponding results are presented in Tab. 2 and Fig. 8. Overall, the proposed model achieved the highest average classification accuracy in this comparison, with a test accuracy of 0.978214 ± 0.002648, which is slightly higher than CNN (0.975), QCNN1 (0.970854 ± 0.006114), QCNN2 (0.960801 ± 0.003847), and QCNN3 (0.977291 ± 0.001770). In addition to the highest mean test accuracy in the reported comparison, the proposed model also maintained a relatively small standard deviation, indicating stable behavior under the current experimental setting.

The competitive performance of the proposed model is closely related to its circuit design. The proposed quantum convolution circuit employs four qubits to represent a 3×3 input region through layered R_Y encoding and progressive entanglement operations. Specifically, the nine normalized values from each local image region are sequentially embedded into the four qubits by repeated R_Y rotations, enabling efficient information loading under limited quantum resources. The subsequent cascaded CNOT operations establish inter-qubit correlations, allowing local features to interact and fuse in the quantum Hilbert space. This design improves the expressive capacity of the quantum convolution kernel while keeping the circuit depth moderate, which is beneficial for stable optimization.

Compared with the reference quantum models, the proposed circuit shows a better balance between feature representation and circuit complexity. Although QCNN3 also achieved competitive performance and the margin between the two models is small, the proposed model obtained a slightly higher average test accuracy, suggesting that the combination of multi-data encoding and structured entanglement can complete convolution-like operations over a 3×3 region and provide useful representations for the subsequent classifier.

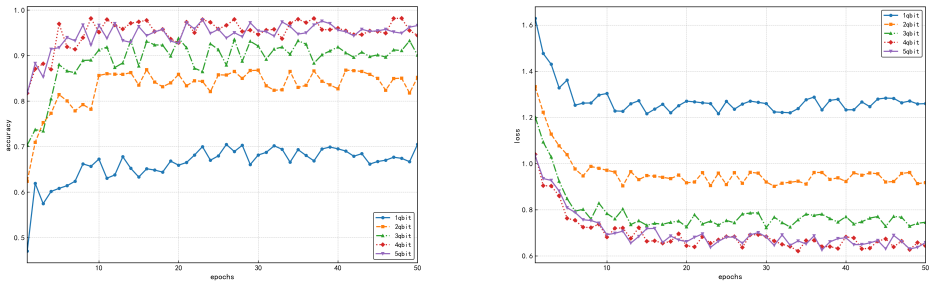
These results support the effectiveness of the proposed quantum convolution architecture for image classification under the current experimental setting. Rather than relying solely on increasing gate number or circuit complexity, the performance gain mainly comes from a more suitable encoding strategy and entanglement pattern. This indicates that, for hybrid quantum-classical models, the design of the quantum convolution struc-

ture is crucial for achieving strong classification accuracy and stable learning performance.

5.2. Impact of Qubit Number

Table 3. Model accuracy and loss curves with different numbers of qubits

model	qubit	gate	size	Accuracy
1qubit	1	9	3×3	0.700770 ± 0.004389
2qubit	2	9	3×3	0.858327 ± 0.008926
3qubit	3	9	3×3	0.933126 ± 0.004351
4qubit	4	12	3×3	0.978214 ± 0.002648
5qubit	5	13	3×3	0.976788 ± 0.001467



(a) accuracy **(b)** loss

Fig. 9. Model accuracy with different numbers of qubits

To investigate the effect of qubit number on convolution performance, we constructed quantum convolution circuits with 1, 2, 3, 4, and 5 qubits. The results in Tab. 3 and Fig. 9 show that model accuracy improves markedly as the number of qubits increases from 1 to 4. Specifically, the test accuracy rises from 0.700770 ± 0.004389 with 1 qubit to 0.858327 ± 0.008926 with 2 qubits and 0.933126 ± 0.004351 with 3 qubits, reaching the best performance of 0.978214 ± 0.002648 with 4 qubits. When the qubit number is further increased to 5, the model still maintains a high accuracy of 0.976788 ± 0.001467, indicating that the proposed design remains effective under slightly higher quantum resources.

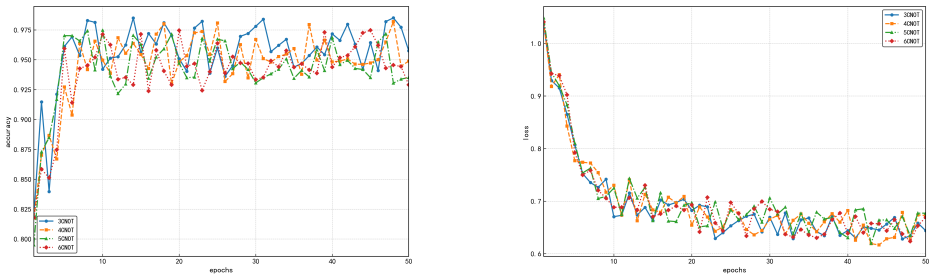
This trend demonstrates that increasing the number of qubits can substantially enhance the feature representation capability of the quantum convolution circuit. With too few qubits, the available quantum state space is limited, making it difficult to capture the complex local patterns contained in the input data. As the number of qubits increases,

the circuit can encode and correlate richer feature information, thereby improving classification performance. Notably, the proposed 4-qubit configuration achieves the highest accuracy among the tested qubit settings while maintaining moderate circuit complexity, showing an effective balance between representation capability and quantum resource consumption. This configuration is not claimed to be theoretically optimal in a universal sense; rather, it is selected as an empirically favorable and resource-balanced setting in the current experiments. These results further confirm that an appropriate qubit configuration is crucial for designing efficient and high-performing quantum convolution models.

5.3. Impact of CNOT Gate Number

Table 4. Impact of CNOT gate number on model performance

model	qubit	gate	size	Accuracy
3CNOT	4	12	3×3	0.978214 ± 0.002648
4CNOT	4	13	3×3	0.978536 ± 0.004719
5CNOT	4	14	3×3	0.973267 ± 0.001665
6CNOT	4	15	3×3	0.974333 ± 0.000365



(a) accuracy **(b)** loss

Fig. 10. Accuracy and loss curves of models under different CNOT gates

Based on the 4-qubit setting, we further investigated the effect of different numbers of CNOT gates on model performance. Specifically, the classification results under 3, 4, 5, and 6 CNOT gates were compared. As shown in Tab. 4 and Fig. 10, the model achieved test accuracies of 0.978214 ± 0.002648, 0.978536 ± 0.004719, 0.973267 ± 0.001665, and 0.974333 ± 0.000365 for 3, 4, 5, and 6 CNOT gates, respectively. Among them, the 4-CNOT configuration obtained the highest mean accuracy, while the proposed 3-CNOT design achieved very competitive performance with lower circuit complexity.

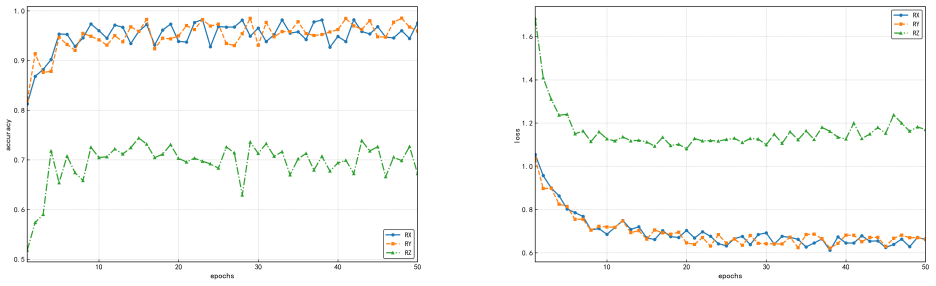
These results indicate that the number of CNOT gates has an important influence on the feature extraction ability of the quantum convolution circuit. A moderate increase in

entanglement can enhance inter-qubit information interaction and improve feature representation, which explains the strong performance of the 3-CNOT and 4-CNOT configurations. However, an excessive number of CNOT gates may introduce redundant interactions and reduce the effectiveness of the circuit. Overall, the results show that an appropriate entanglement depth is essential for achieving strong classification performance, and that the proposed 3-CNOT structure provides an effective balance between accuracy and circuit efficiency.

5.4. Impact of Encoding Gates

Table 5. Impact of encoding gates on model performance

model	qubit	gate	size	Accuracy
rx	4	12	3×3	0.976858 ± 0.003890
ry	4	12	3×3	0.978214 ± 0.002648
rz	4	16	3×3	0.726865 ± 0.012067



(a) accuracy **(b)** loss

Fig. 11. Accuracy and loss curves of models with different encoding gates

The choice of encoding gate has a clear influence on the performance of the quantum convolutional model. To evaluate this effect, we compared three encoding strategies based on R_X, R_Y, and R_Z gates under the same 4-qubit setting. As shown in Tab. 5 and Fig. 11, the proposed R_Y-based encoding achieved the best test accuracy of 0.978214 ± 0.002648, while R_X encoding also showed competitive performance with an accuracy of 0.976858 ± 0.003890. In contrast, the performance of R_Z encoding dropped markedly to 0.726865 ± 0.012067, indicating a much weaker feature representation capability in the current circuit design.

These results suggest that the encoding strategy should be matched carefully with the circuit structure and measurement process. In the proposed quantum convolution circuit,

R_Y encoding provides a more effective way to map classical information into quantum states and supports subsequent entanglement-based feature extraction, leading to the best overall classification performance. Although R_X encoding also performs well, its accuracy is slightly lower than that of R_Y, indicating that the proposed R_Y-based design is better suited to the present architecture. By comparison, R_Z encoding mainly introduces phase variation and is less effective in producing discriminative feature representations under the current setting. Overall, the results confirm that the proposed R_Y encoding strategy is more suitable for the designed quantum convolution model.

6. Evaluation and Analysis

In this section, we further analyze the proposed method based on the experimental results.

We first compared the proposed quantum convolution model with a classical CNN and three reference quantum convolution models. The results show that the proposed model achieved the best test accuracy of 0.978214 ± 0.002648, which is slightly higher than CNN (0.975), QCNN1 (0.970854 ± 0.006114), QCNN2 (0.960801 ± 0.003847), and QCNN3 (0.977291 ± 0.001770). These results indicate that the proposed circuit design can effectively improve feature extraction and classification performance while maintaining good stability.

To further investigate the effect of qubit number, we constructed quantum convolution circuits with 1, 2, 3, 4, and 5 qubits. The results show that test accuracy increases from 0.700770 ± 0.004389 to 0.858327 ± 0.008926 and 0.933126 ± 0.004351 as the number of qubits grows from 1 to 3, and reaches the best value of 0.978214 ± 0.002648 at 4 qubits. When the number of qubits is further increased to 5, the model still maintains a high accuracy of 0.976788 ± 0.001467. This trend shows that increasing the number of qubits can substantially enhance the feature representation ability of the quantum circuit, while the 4-qubit configuration provides the most favorable balance between performance and resource cost.

We also analyzed the influence of the number of CNOT gates under the 4-qubit setting. The corresponding accuracies with 3, 4, 5, and 6 CNOT gates are 0.978214 ± 0.002648, 0.978536 ± 0.004719, 0.973267 ± 0.001665, and 0.974333 ± 0.000365, respectively. The results indicate that a moderate entanglement depth is beneficial for inter-qubit information interaction and feature fusion. Although the 4-CNOT configuration achieved the highest mean accuracy, the proposed 3-CNOT design produced highly competitive performance with lower circuit complexity, showing that an appropriate entanglement structure is more important than simply increasing the number of entangling gates.

In addition, the choice of encoding gate has a clear impact on model performance. Under the same 4-qubit setting, the proposed R_Y-based encoding achieved the best test accuracy of 0.978214 ± 0.002648, while R_X encoding also showed competitive performance with 0.976858 ± 0.003890. In contrast, R_Z encoding dropped sharply to 0.726865 ± 0.012067. These results suggest that the encoding strategy should be carefully matched with the circuit structure and measurement process. In the proposed model, R_Y encoding is better suited to the current quantum convolution architecture and provides more effective feature representation.

Overall, the experimental results demonstrate that the proposed quantum convolution kernel achieves strong classification performance through a balanced design of qubit num-

ber, entanglement depth, and encoding strategy. Rather than relying on a larger number of gates, the improvement mainly comes from a more suitable circuit structure, which confirms the effectiveness of the proposed method for quantum-enhanced image feature extraction.

7. Concluding Remarks and Future Directions

This work proposes a hybrid quantum-classical convolutional neural network based on a quantum convolution kernel for image classification. The model employs a four-qubit quantum circuit with layered encoding and CNOT-based entanglement to perform convolution-like operations on local image regions, followed by classical classification. This design improves feature representation capability while maintaining relatively low quantum resource consumption.

Experimental results support the effectiveness of the proposed model under the current proof-of-concept setting. Compared with CNN and three reference quantum convolution models, the proposed method achieved the highest average test accuracy of 0.978214 ± 0.002648. Further controlled experiments show that the number of qubits, the number of CNOT gates, and the choice of encoding gate all have important effects on performance. In particular, the 4-qubit configuration provided the best balance between accuracy and resource efficiency, the proposed 3-CNOT design maintained competitive performance with reduced circuit complexity, and the R_Y encoding strategy achieved the best overall results under the current circuit structure.

These findings indicate that the performance of hybrid quantum neural networks can be improved through careful quantum circuit design. Since the experiments are conducted on a reduced MNIST subset and a simulator-level noisy environment, the results should be interpreted as a proof-of-concept evaluation rather than a complete demonstration of scalability to large-scale image classification tasks or deployment on real quantum hardware. Nevertheless, the results suggest that the proposed quantum convolution architecture provides a compact and potentially useful scheme for image feature extraction under limited quantum resources.

In future work, we will further explore more flexible encoding strategies and circuit structures, evaluate the proposed model on larger and more complex datasets, and investigate its deployment on real quantum hardware. In addition, integrating the current quantum convolution design with other quantum modules may provide a promising direction for building more powerful hybrid quantum learning architectures.

Acknowledgement. This work was supported by the National Natural Science Foundation of China (Grant No. 62372168), National Key R&D Program of China (No.2023YFC2811102), the Open Project of the Key Laboratory of Artificial Intelligence and Information Processing, Education Department of Guangxi Zhuang Autonomous Region (Hechi University) (Grant No. 2024GXZDSY010), Hunan Province Science and Technology Innovation Plan Project (No. 2023ZJ1020), and the Hunan Provincial Postgraduate Scientific Research Innovation Projects (Grant Nos. LXBZZ2024276 and CX20251547).

References

1. Liao, J., Guo, L., Jiang, L., Yu, C., Liang, W., Li, K., Pop, F.: A machine learning-based feature extraction method for image classification using ResNet architecture. Digital Signal Processing 160, 105036 (2025)
2. Diao, C., Zhang, D., Liang, W., Jiang, M., Li, K.: A novel attention-based dynamic multi-graph spatial-temporal graph neural network model for traffic prediction. IEEE Transactions on Emerging Topics in Computational Intelligence 9(2), 1910–1923 (2024)
3. Hu, N., Zhang, D., Xie, K., Liang, W., Li, K.C., Zomaya, A.Y.: Multi-graph fusion based graph convolutional networks for traffic prediction. Computer Communications 210, 194–204 (2023)
4. Dayarathna, S., Islam, K.T., Uribe, S., Yang, G., Hayat, M., Chen, Z.: Deep learning based synthesis of MRI, CT and PET: Review and analysis. Medical Image Analysis 92, 103046 (2024)
5. Archana, R., Jeevaraj, P.S.E.: Deep learning models for digital image processing: A review. Artificial Intelligence Review 57(1), 11 (2024)
6. Shi, Y., Li, Q., Zhu, X.X.: Building segmentation through a gated graph convolutional neural network with deep structured feature embedding. ISPRS Journal of Photogrammetry and Remote Sensing 159, 184–197 (2020)
7. Cong, I., Choi, S., Lukin, M.D.: Quantum convolutional neural networks. Nature Physics 15(12), 1273–1278 (2019)
8. Brady, L.T., Baldwin, C.L., Bapat, A., Kharkov, Y., Gorshkov, A.V.: Optimal protocols in quantum annealing and quantum approximate optimization algorithm problems. Physical Review Letters 126(7), 070505 (2021)
9. Herrmann, J., Llima, S.M., Remm, A., Zapletal, P., McMahon, N.A., Scarato, C., Swiadek, F., Andersen, C.K., Hellings, C., Krinner, S., Lacroix, N., Lazar, S., Kerschbaum, M., Zanuz, D.C., Norris, G.J., Hartmann, M.J., Wallraff, A., Eichler, C.: Realizing quantum convolutional neural networks on a superconducting quantum processor to recognize quantum phases. Nature Communications 13, 4144 (2022)
10. Fellous-Asiani, M., Chai, J.H., Whitney, R.S., Auffèves, A., Ng, H.K.: Limitations in quantum computing from resource constraints. PRX Quantum 2(4), 040335 (2021)
11. Lü, W., Lu, Y., Li, J., Sigov, A., Ratkin, L., Ivanov, L.A.: Quantum machine learning: classifications, challenges, and solutions. Journal of Industrial Information Integration 42, 100736 (2024)
12. Gheorghiu, V., Mosca, M.: Quantum resource estimation for large scale quantum algorithms. Future Generation Computer Systems 162, 107480 (2025)
13. Pan, J.: Reducing qubit budget in quantum machine learning. Nature Computational Science 1(9), 565 (2021)
14. Su, J., Guo, X., Liu, C., Li, L.: A new trend of quantum image representations. IEEE Access 8, 214520–214537 (2020)
15. Ovalle-Magallanes, E., Aviña-Cervantes, J.G., Cruz-Aceves, I., Ruiz-Pinales, J.: Hybrid classical-quantum convolutional neural network for stenosis detection in X-ray coronary angiography. Expert Systems with Applications 189, 116112 (2022)
16. Huang, R., Tan, X., Xu, Q.: Learning to learn variational quantum algorithm. IEEE Transactions on Neural Networks and Learning Systems 34(11), 8430–8440 (2022)
17. Zheng, J., Gao, Q., Lü, J., Ogorzałek, M., Pan, Y., Lü, Y.: Design of a quantum convolutional neural network on quantum circuits. Journal of the Franklin Institute 360(17), 13761–13777 (2023)
18. Caro, M.C., Huang, H.Y., Cerezo, M., Sharma, K., Sornborger, A., Cincio, L., Coles, P.J.: Generalization in quantum machine learning from few training data. Nature Communications 13, 4919 (2022)

19. Pan, F., Chen, K., Zhang, P.: Solving the sampling problem of the Sycamore quantum circuits. Physical Review Letters 129(9), 090502 (2022)
20. Tang, H., Li, B., Wang, G., Xu, H., Li, C., Barr, A., Cappellaro, P., Li, J.: Communication-efficient quantum algorithm for distributed machine learning. Physical Review Letters 130(15), 150602 (2023)
21. Zhou, M.G., Cao, X.Y., Lu, Y.S., Wang, Y., Bao, Y., Jia, Z.Y., Fu, Y., Yin, H.L., Chen, Z.B.: Experimental quantum advantage with quantum coupon collector. Research p. 9798679 (2022)
22. Lu, X., Pan, K., Yan, G., Shan, J., Wu, W., Yan, J.: QAS-bench: Rethinking quantum architecture search and a benchmark. In: Proceedings of the 40th International Conference on Machine Learning. Proceedings of Machine Learning Research, vol. 202, pp. 22880–22898. PMLR, Honolulu, Hawaii, USA (2023), https://proceedings.mlr.press/v202/lu23f.html
23. Zhou, M.G., Liu, Z.P., Yin, H.L., Li, C.L., Xu, T.K., Chen, Z.B.: Quantum neural network for quantum neural computing. Research 6, 0134 (2023)
24. Meng, Y.M., Zhang, J., Zhang, P., Gao, C., Ran, S.J.: Residual matrix product state for machine learning. SciPost Physics 14(6), 142 (2023)
25. Wu, S., Zhang, Y., Li, J.: Quantum data parallelism in quantum neural networks. Physical Review Research 7(1), 013177 (2025)
26. Fan, F., Shi, Y., Guggemos, T., Zhu, X.X.: Hybrid quantum-classical convolutional neural network model for image classification. IEEE transactions on neural networks and learning systems 35(12), 18145–18159 (2023)
27. Li, Y., Zhou, R.G., Xu, R., Luo, J., Hu, W.: A quantum deep convolutional neural network for image recognition. Quantum Science and Technology 5(4), 044003 (2020)
28. Okmi, M., Por, L.Y., Ang, T.F., Al-Hussein, W., Ku, C.S.: A systematic review of mobile phone data in crime applications: A coherent taxonomy based on data types and analysis perspectives, challenges, and future research directions. Sensors 23(9), 4350 (2023)
29. Ku, C.S., Xiong, J., Chen, Y.L., Cheah, S.D., Soong, H.C., Por, L.Y.: Improving stock market predictions: An equity forecasting scanner using long short-term memory method with dynamic indicators for malaysia stock market. Mathematics 11(11), 2470 (2023)
30. He, Z., Yang, J., Alroobaea, R., Por, L.Y.: Seizurelstm: An optimal attention-based trans-lstm network for epileptic seizure detection using optimal weighted feature integration. Biomedical Signal Processing and Control 96, 106603 (2024)
31. Taherinavid, S., Moravvej, S.V., Chen, Y.L., Yang, J., Ku, C.S., Por, L.Y.: Automatic transportation mode classification using a deep reinforcement learning approach with smartphone sensors. IEEE Access 12, 514–533 (2024)
32. Hu, N., Zhang, D., Xie, K., Liang, W., Diao, C., Li, K.C.: Multi-range bidirectional mask graph convolution based GRU networks for traffic prediction. Journal of Systems Architecture 133, 102775 (2022)
33. Diao, C., Zhang, D., Liang, W., Li, K.C., Hong, Y., Gaudiot, J.L.: A novel spatial-temporal multi-scale alignment graph neural network security model for vehicles prediction. IEEE Transactions on Intelligent Transportation Systems 24(1), 904–914 (2023)
34. Liu, J., Lim, K.H., Wood, K.L., Huang, W., Guo, C., Huang, H.L.: Hybrid quantum-classical convolutional neural networks. Science China Physics, Mechanics & Astronomy 64(9), 290311 (2021)
35. Yang, C.H.H., Qi, J., Chen, S.Y.C., Chen, P.Y., Siniscalchi, S.M., Ma, X., Lee, C.H.: Decentralizing feature extraction with quantum convolutional neural network for automatic speech recognition. In: ICASSP 2021 - 2021 IEEE International Conference on Acoustics, Speech and Signal Processing (ICASSP). pp. 6523–6527. IEEE, Toronto, ON, Canada (2021)

Xiaoliang Wang is a professor of information technology and chair of the Department of Internet of Things Engineering, Hunan University of Science and Technology. He leads a

team of researchers and students in Information Security and the Internet of Things, such as VANET security and Anonymous Authentication in Ad Hoc Networks. He received a B.E. in computer engineering from Xiangtan University, China, and an M.S. in computer science from the joint education of Xiangtan University and the Institute of Computing Technology of the Chinese Academy of Sciences, China. He received his Ph.D. from Hunan University. He had worked at Xiangtan University and the Nanjing Government of China and had also worked as a postdoctoral researcher at the University of Alabama.

Lianghai Chen is currently pursuing a Master's degree in Computer Science and Technology at Hunan University of Science and Technology. He received his Bachelor's degree in Computer Science and Technology in 2023. His research interests include Quantum Computing and Computer Vision (CV).

Yi Lu is currently pursuing a Master's degree in Software Engineering at Hunan University of Science and Technology. She received her Bachelor's degree in Computer Science and Technology in 2024. Her research interests include Emotional Brain-Computer Interfaces (EBCI) and Computer Vision (CV).

Liang Bai is a specially appointed associate professor at the School of Computer Science and Engineering, Hunan University of Science and Technology, China. He received his Ph.D. degree from Hunan University in 2025, his M.E. degree in Software Engineering from Hunan University of Science and Technology in 2020, and his B.E. degree in Information Management and Information Systems from Hengyang Normal University in 2014. His research interests include graph deep learning, large language models, single-cell data mining, single-cell cell–cell communication analysis, and Internet of Vehicles (IoV) security. He has published over 10 papers in highly indexed journals and flagship conferences. He serves as a regular reviewer for journals such as IEEE/ACM Transactions on Computational Biology and Bioinformatics and BMC Bioinformatics, and has been a PC member of IEEE BIBM. He has actively participated in several major national research projects, including the National Key R&D Program of China and key projects of the National Natural Science Foundation of China.

Huaning Song is an associate professor at Hechi University and the vice dean of the School of Artificial Intelligence and Manufacturing. He is also one of the main members of the Key Laboratory of AI and Information Processing under the Education Department of the Guangxi Zhuang Autonomous Region. He specializes in the application of artificial intelligence models and the development of embedded technologies. He graduated from Guilin University of Electronic Technology with a master's degree in circuits and systems.

Kuanching Li is a professor at the School of Computer Science and Engineering, Hunan University of Science and Technology. Dr. Li has co-authored over 150 conference and journal papers, holds several patents, and serves as an associate and guest editor for various scientific journals. He has also held chair positions at several prestigious international conferences. His research interests include cloud and edge computing, big data, and blockchain technologies. Dr. Li is a Fellow of the Institution of Engineering and Technology (IET).

Received: April 11, 2026; Accepted: August 17, 2026.